Biomaterials Science

ROYAL SOCIETY OF CHEMISTRY

PAPER

View Article Online
View Journal | View Issue

Cite this: *Biomater. Sci.*, 2020, **8**, 5196

Ciprofloxacin-loaded bioadhesive hydrogels for ocular applications†

Islam A. Khalil,[a,b,c,d] Bahram Saleh,[a] Dina M. Ibrahim,[a,e] Clotilde Jumelle,[f] Ann Yung,[f] Reza Dana[f] and Nasim Annabi *[b,c,g]

The management of corneal infections often requires complex therapeutic regimens involving the prolonged and high-frequency application of antibiotics that provide many challenges to patients and impact compliance with the therapeutic regimens. In the context of severe injuries that lead to tissue defects (*e.g.* corneal lacerations) topical drug regimens are inadequate and suturing is often indicated. There is thus an unmet need for interventions that can provide tissue closure while concurrently preventing or treating infection. In this study, we describe the development of an antibacterial bioadhesive hydrogel loaded with micelles containing ciprofloxacin (CPX) for the management of corneal injuries at risk of infection. The *in vitro* release profile showed that the hydrogel system can release CPX, a broad-spectrum antibacterial drug, for up to 24 h. Moreover, the developed CPX-loaded hydrogels exhibited excellent antibacterial properties against *Staphylococcus aureus* and *Pseudomonas aeruginosa*, two bacterial strains responsible for the most ocular infections. Physical characterization, as well as adhesion and cytocompatibility tests, were performed to assess the effect of CPX loading in the developed hydrogel. Results showed that CPX loading did not affect stiffness, adhesive properties, or cytocompatibility of hydrogels. The efficiency of the antibacterial hydrogel was assessed using an *ex vivo* model of infectious pig corneal injury. Corneal tissues treated with the antibacterial hydrogel showed a significant decrease in bacterial colony-forming units (CFU) and a higher corneal epithelial viability after 24 h as compared to non-treated corneas and corneas treated with hydrogel without CPX. These results suggest that the developed adhesive hydrogel system presents a promising suture-free solution to seal corneal wounds while preventing infection.

Received 7th June 2020,
Accepted 29th July 2020

DOI: 10.1039/d0bm00935k

rsc.li/biomaterials-science

Introduction

Ocular injuries, one of the leading threats to vision worldwide, represent a huge burden for healthcare systems with 1.5–2 million new cases annually in the United States.[1] Spanning from superficial abrasions to full-thickness perforations, these injuries result from a variety of causes including blunt force injuries, penetration of foreign bodies, chemical burns, among others. Ocular injuries are associated with a high risk of infection due to breakdown of the main barrier against infection, the superficial epithelium that lines the eye, which may also include rupture of the cornea or sclera, permitting infiltration of microorganism into the eye.[2] While superficial injuries can usually self-heal, more severe eye injuries require surgical intervention including suturing, use of adhesives/sealants, or tissue grafting (amniotic membrane or corneal tissue). Standard post-injury treatment regimens include antibiotics that are topically instilled on the eye surface. Nevertheless, eye drops have shown low efficacy due to short contact time on the ocular surface (within 1–2 min), limiting drug bioavailability.[3] Moreover, eye drop application is

[a]*Department of Chemical Engineering, Northeastern University, Boston, MA, USA*
[b]*Brigham and Women's Hospital, Harvard Medical School, Boston, MA, USA*
[c]*Harvard-MIT Division of Health Sciences and Technology, Massachusetts Institute of Technology, Cambridge, MA, USA*
[d]*Department of Pharmaceutics, Misr University of Science and Technology, 6th of October City 12566, Giza, Egypt*
[e]*Energy Materials Laboratory, School of Sciences and Engineering, The American University in Cairo, New Cairo 11835, Egypt*
[f]*M; assachusetts Eye and Ear, Department of Ophthalmology, Harvard Medical School, Boston, MA, USA*
[g]*Department of Chemical and Biomolecular Engineering, University of California, Los Angeles, Los Angeles, CA 90095, USA. E-mail: nannabi@ucla.edu; Tel: +1(310) 267-5927*

†Electronic supplementary information (ESI) available: Materials and methods for characterization of CPX-loaded MCs, *in vitro* release study of CPX-loaded MCs, *in vitro* antimicrobial study on CPX-loaded MCs, ^{1}H NMR analysis, mechanical characterization of MCs-loaded GelCORE hydrogels, swelling and degradation characterization of MCs-loaded GelCORE hydrogels, and adhesion tests on MCs-loaded GelCORE hydrogels. Also, Supplementary Fig. 1. Development of GelCORE + MCs bioadhesives, and Supplementary Fig. 2. *In vitro* characterization of MCs-loaded GelCORE hydrogels. See DOI: 10.1039/d0bm00935k

further limited as it has been estimated that 9 out of 10 patients are unable to instill eye drops correctly.[4] Ointments can be used with a low frequency of administration (*e.g.* every 4–6 hours) but can cause visual blurring and delayed injury healing. These limitations highlight the need for new drug delivery systems to better prevent infection of eye injuries.

A potential alternative to a frequent topical application would be to combine medical devices used for wound closure, such as sutures or adhesives/sealants, with drugs. Accordingly, antibiotic-eluting sutures have been developed and are now commercially available.[5,6] However, suturing can induce regular and irregular astigmatism as well as corneal neovascularization and also serve as a nidus for microbial growth.[7] The use of fibrin glue, a blood-derived biological adhesive, mixing with antimicrobial peptides, or diverse antibiotics (vancomycin, gentamycin, *etc*.) has been described in the literature.[8,9] However, fibrin-based adhesives have a limited adhesiveness on wet ocular tissues and have low mechanical strength, limiting its efficiency for the closure of eye injuries. Another study reported the infusion of cyanoacrylate glue with antibacterial silver nanoparticles.[10] However, cyanoacrylate glue is well-known for its cytotoxicity and rough surface post-application, leading to inflammation, neovascularization, and opacification of the cornea.[11]

In our previous study, we described the development of a photocrosslinkable gelatin-based bioadhesive, called GelCORE (Gel for Corneal Regeneration), for the sealing and repair of defects and ulcers, protecting the cornea from inflammation, infection or immune disorders.[12] We showed that the bioadhesive can be photocrosslinked on the cornea using visible light to form as an adhesive hydrogel with mechanical properties close to the native corneal tissue. In this study, we aim to further investigate the capability of GelCORE in the prevention of eye infection by loading micelles (MCs) containing ciprofloxacin (CPX), a broad-spectrum antibiotic, within the bioadhesive.

CPX is a second-generation fluoroquinolone antibiotic commonly used in eye drops or ointments to treat bacterial infections or ulcers in the eye.[13] CPX acts as an inhibitor of enzymes required for bacterial DNA synthesis.[14] The solubility of CPX is highly dependent on the aqueous pH due to proton transfer from the carboxylic acid group and to the basic piperazine ring.[15] While CPX is freely soluble in water at acidic pH (4.5), its poor solubility at physiological pH (7.4) results in the formation of crystalline deposits.[16] To address this issue, the encapsulation of CPX in nanocarriers has widely been described, especially for the formulation of eye drops.[17–21] Among these nanocarriers, Pluronic® F127 (PL127), an FDA-approved synthetic, nonionic, and amphiphilic triblock copolymer, has been used as a micellar system for CPX encapsulation and has shown its ability to prevent CPX crystallization at physiologic pH.[17]

In this study, we first described the development and characterization of CPX-loaded MCs including particles' size and charge, encapsulation efficiency, drug loading, morphology, thermal behavior, drug release, and antimicrobial properties. The optimized formulation of the MCs was then incorporated into GelCORE formulation to form an antibacterial bioadhesive hydrogel. *In vitro* release kinetic of CPX from the bioadhesive hydrogel was assessed. Additionally, *in vitro* characterization of physical, mechanical, and antimicrobial properties, as well as cytocompatibility of MC-loaded GelCORE hydrogels was evaluated. Finally, an *ex vivo* model of infectious pig corneal injury was used to study the efficiency of the MC-loaded GelCORE hydrogels for the treatment of the infected eye.

Experimental

Materials

Ciprofloxacin hydrochloride (CPX), Pluronic® F-127 (PL127), Tween 20, methacrylic anhydride Triethanolamine (TEA), *N*-vinylcaprolactam (VC), Eosin Y disodium salt and gelatin (porcine skin, gel strength ≈300 g Bloom, Type A) were purchased from Sigma Aldrich. All solvents were analytical grade and supplied by Sigma Aldrich or Fisher scientific. All cell culture materials were provided by Sigma Aldrich. PrestoBlue assay was obtained from Thermo Fisher Scientific. LIVE/DEAD kit was purchased from Invitrogen. Porcine eyeballs were purchased from Sierra Medical.

Synthesis and characterization of CPX-loaded MCs

CPX-loaded MCs were prepared using a nanoprecipitation technique previously reported.[22] Briefly, different ratios of CPX and Pluronic F-127 (PL127) were dissolved in a solvent mixture (dimethyl sulfoxide (DMSO) : acetone 1 : 4) supplemented with 2% (v/v) of triethanolamine (TEA). The organic phase was added dropwise to Dulbecco's Phosphate Buffered Saline (DPBS) at a ratio of 1 : 2 (v/v) while stirring at 300 rpm at room temperature to form MCs. The colloid solution was then agitated until complete evaporation of the organic solvent (acetone) and centrifuged at 14 000 rpm for 30 min to separate MCs from the DMSO and the un-entrapped drug molecules. The pellets were suspended in DPBS followed by lyophilization. The prepared CPX-loaded MCs were referenced as MCs (1 : 2), MCs (1 : 6), and MCs (1 : 10) according to CPX to PL127 ratios. CPX-loaded MCs were characterized using dynamic light scattering analyzer (Nano-ZS90 Zetasizer, Malvern Instruments, UK), UV–Vis spectrophotometer (Shimadzu UV 1650 Spectrophotometer, Japan), scanning electron microscope (SEM) (Hitachi S-4800 scanning electron microscope), and differential scanning calorimetry (DSC) analysis (Q20, TA instrument, MA, USA) (ESI, S1.1†).

In vitro release study of CPX-loaded MCs

The *in vitro* release of free CPX and CPX-loaded MCs in DPBS was determined by using a dialysis membrane technique.[23] A 0.05% Tween 20 solution in DPBS (pH 7.4) was used to mimic ocular surface environment pH and to maintain sink conditions during the experiments (ESI, S1.2†).

In vitro antimicrobial study on CPX-loaded MCs

Minimum inhibitory concentrations (MICs) for both *Staphylococcus aureus* (ATCC® 29213™) and *Pseudomonas aeruginosa* (ATCC® 15692™) were determined by a microdilution test.[14] MIC is the lowest antimicrobial concentration inhibiting microorganism growth after incubating the drug with microorganisms (ESI, S1.3†).

Preparation of MCs-loaded GelCORE hydrogels

GelCORE hydrogels were engineered by using gelatin methacryloyl (GelMA) and a photoinitiator solution as described in our previous study.[12] To synthesize GelMA, 10 g of porcine gelatin was dissolved in 100 ml of DPBS and heated at 60 °C for 1 h. Next, 8 ml of methacrylic anhydride was added dropwise to the gelatin solution under continuous stirring at 50 °C for 3 h. The solution was then dialyzed for 5 days to remove unreacted methacrylic anhydride and then placed in a −80 °C freezer for 24 h. The frozen polymer was then freeze-dried for 5 days.

The photoinitiator solution was prepared by dissolving TEA (1.8% (w/v)), *N*-vinylcaprolactam (VC) (1.25% (w/v)) and Eosin Y disodium salt (0.5 mM) in distilled water. A precursor solution was then prepared by dissolving 20% (w/v) of GelMA and 11% (w/v) of CPX-loaded MCs in the photoinitiator solution and vortexed at 37 °C, where CPX amount represented the equivalent dose for two days to prevent bacterial infection. To prepare a hydrogel sample, 70 μL of this precursor solution was placed into polydimethylsiloxane (PDMS) cylindrical molds (diameter: 6 mm; height: 2.5 mm) or rectangular molds (14 × 5 × 1 mm). The solution was finally photocrosslinked *via* exposure to visible light (480–520 nm) using a LS1000 Focal Seal Xenon Light Source (100 mW cm^{-2}, Genzyme) for 4 min. SEM analysis was used to observe the porosity of the crosslinked hydrogels using a Hitachi S-4800 Scanning Electron Microscope. Proton nuclear magnetic resonance (^{1}H NMR) was used to confirm methacrylation of gelatin as described in previous studies[12,24] (ESI, S1.4†). Mechanical, swelling, and degradation properties of MC-loaded GelCORE hydrogels were tested, more details in (ESI, S1.5 and 6†).

In vitro release kinetics studies on MCs-loaded GelCORE hydrogels

The *in vitro* release of CPX from MC-loaded GelCORE adhesive was studied in DPBS with 0.05% Tween 20 using the dialysis membrane technique as previously mentioned in *in vitro* release study for CPX-loaded MCs. In this test, MCs-loaded GelCORE suspended immersed in 1 mL release media and transferred into donor compartments covered with dialysis membranes.

Adhesion tests on MCs-loaded GelCORE hydrogels

The adhesive properties MC-loaded GelCORE hydrogels were tested using different standardized tests, including burst pressure test on collagen sheets, corneal tissue and rabbit eyeballs, and wound closure test (ESI, S1.7†).

In vitro antimicrobial study on MCs-loaded GelCORE hydrogels

For the *in viro* antimicrobial tests, different bioadhesives with/without CPX-loaded MCs were first prepared as described previously followed by sterilization, where hydrogel sample was exposed to UV light (302 nm) for 5 min.

Preparation of bacterial inocula

Gram-positive *Staphylococcus aureus* (ATCC® 29213™) and Gram-negative *Pseudomonas aeruginosa* (ATCC® 15692™) were used as model microbial strains. A single colony of each bacteria strain was inoculated in 5 mL of tryptic soy broth (TSB, Sigma) and incubated overnight in a bacterial shaker incubator (200 rpm at 37 °C). The optical density (OD) of the resulting bacterial suspension was adjusted to an OD of 0.52 (10^9 CFU ml^{-1}) at a wavelength of 562 nm using a spectrophotometer. Bacterial inocula were prepared by diluting the suspension to a final concentration of 10^6 CFU ml^{-1}.

Agar diffusion test

100 μl of bacterial inocula of each strain (10^6 CFU ml^{-1}) was spread on 6 mm diameter tryptic soy agar plates. CPX, MCs, and GelCORE with/without MCs (previously sterilized by UV light) were placed on the plates. 24 h after incubation at 37 °C, the inhibition zone for each sample was measured. Each sample was tested in triplicate.

Bacterial viability assay

CPX, MCs, and GelCORE hydrogel samples with and without MCs were incubated in 1 ml of the bacterial inocula at 37 °C and 5% CO_2 for 24 h. After incubation, hydrogel samples were carefully rinsed three times with DPBS to remove bacteria on the surface. After washing, a commercial LIVE/DEAD® BacLight™ kit was used to determine bacterial cell viability in the bacterial inocula. Fluorescently stained samples were imaged using a Zeiss Axio Observer Z1 inverted microscope. Each sample was tested in triplicate.

In vitro cytocompatibility studies

Cell line. A corneal fibroblast cell line (ATCC) was used to assess the effect of loading MCs on the cytocompatibility of GelCORE hydrogels. Cells were cultured at 37 °C and 5% CO_2 in Dulbecco's Modified Eagle Media (DMEM) with Nutrient Mixture F-12 (DMEM/NM-F12) supplemented with 10% (v/v) FBS, 1% (v/v) penicillin/streptomycin, and 1% (v/v) L-glutamine. Cells were cultured in tissue culture flasks and passaged at 70% confluency.

2D cell seeding on hydrogel. 7 μL of prepolymer solution (GelCORE or MCs-loaded GelCORE) was added on 3-(trimethoxysilyl) propyl methacrylate (TMSPMA)-coated glass slides and photocrosslinked for 4 min *via* visible light while maintaining 300 μm thickness. On top of the crosslinked hydrogel sample, 40 μL of cell solution (2 × 10^6 cells per mL) was added, incubated for 45 min, diluted with 360 μL of cell culture media, and incubated at 37 °C and 5% CO_2 for 5 days.

2D cell viability. Viability of corneal fibroblast cells was monitored by staining cells with calcein-AM and ethidium homodimer-1 (LIVE/DEAD kit).[12] Briefly, the staining solution was prepared by mixing 0.5 μL calcein-AM and 2 μL ethidium homodimer-1 in 1 mL of DPBS. For each bioadhesive sample, the cell medium was replaced with 100 μL of staining solution and incubated for 15 min at 37 °C. Fluorescent images were acquired by ZEISS (AxioObserver Z1) and analyzed by ImageJ software.

2D cell adhesion and spreading. Spreading of corneal fibroblasts was monitored by F-actin (for microfilaments) and DAPI (for cell nuclei) staining.[12] Briefly, unattached cells were washed from the samples by DPBS, followed by fixation for 20 min using a 4% (v/v) paraformaldehyde solution. The samples were washed three times with DPBS. A 0.1% (w/v) Triton X-100 solution in DPBS was added to fixed samples for 20 min to permeabilize the cell membrane. The samples were washed three times with DPBS. A 1.25% (v/v) of Alexa Fluor 488-labeled phalloidin solution in 0.1% BSA was used to stain cell actin filaments for 45 min, followed by adding DAPI (1 μL mL^{-1}) in DPBS for 5 min to stain cell nuclei. Fluorescent images were acquired by ZEISS (AxioObserver Z1).

2D cell proliferation. The metabolic activity of corneal fibroblasts was measured using a PrestoBlue assay.[12] Briefly, 10% (v/v) PrestoBlue dye was added to cell-seeded samples on post-incubation days 1, 4, and 7, followed by incubation for 1 h at 37 °C. Fluorescence intensity of the resulting solutions was measured at 535–560 nm excitation and 590–615 nm emission (BioTek Synergy LX, USA).

Ex vivo efficiency studies on MCs-loaded GelCORE hydrogels

Organ culture infectious model. We used an *ex vivo* organ culture infectious model based on the previously described protocols.[25–27] *Pseudomonas aeruginosa* bacteria were obtained from the American Type Culture Collection (ATCC 27853). Bacteria were grown on TSA plates at 37 °C for 24 h. From the plate, a single colony was inoculated in 5 mL of TSB for 3.5 h (to the end of the exponential growth phase) at 37 °C under agitation. The OD of bacteria was determined using a spectrophotometer set at 600 nm. Inocula were prepared by suspending bacteria in DPBS to a concentration of ~10^6 CFU mL^{-1}. Fresh (harvested within 48 h) pig eyeballs were purchased from Sierra for Medical Science. After removal of extraocular muscles and conjunctival tissue, eyeballs were decontaminated for 1 min in 2.5% povidone–iodine solution and rinsed with DPBS. A partial trephination of approximately 50% corneal depth was created on the central cornea using a 6 mm corneal trephine. A crescent knife was then used to dissect the anterior lamella of the trephined portion. Corneas were then excised with approximately 4 mm of the limbal conjunctiva and placed on concave silicon support, epithelial side down. The endothelial side was filled with 2%-agar (Sigma) Dulbecco's Modified Eagle's medium (DMEM; Sigma) supplemented with 10% Fetal Bovine Serum (FBS; Atlanta Biologicals, Flowery Branch, GA). Once the agar solidified, corneas were placed in a Petri dish, epithelial side up, and DMEM, supplemented with 10% FBS, was added until the limbus, leaving the epithelium exposed to air. Subsequently, 10 μL of the bacterial inoculum was inoculated directly on the corneal defect, corresponding to a final concentration of ~10^4 CFU per cornea. Corneas were then incubated in a humidified 5% CO_2 incubator at 37 °C.

Hydrogel application. 24 h after bacterial inoculation, corneas were divided into three groups (n = 6 per group). For the control group, no bioadhesive was applied to the defect. For the two other groups, 20 μL of GelCORE or GelCORE + MCs precursor solution was used to fill the defect. Precursor solutions were photopolymerized for 4 min with visible light until complete solidification. For all groups, corneas were then incubated in a humidified 5% CO_2 incubator at 37 °C. Optical Coherence Tomography (OCT) imaging of corneas was performed before and after the hydrogel application.

Assessment of antibacterial efficiency. The antibacterial efficiency was assessed by CFU counting in the corneal tissue (n = 5) 24 h after hydrogel application. Central corneas were harvested using an 8 mm surgical trephine. Corneas were then cut into small pieces and digested in DMEM containing 0.5% collagenase D (Sigma) at 37 °C for 2 h under agitation. Then, corneas were triturated using a homogenizer for 30 s. After cornea solutions were filtered using a sterile cell strainer (70 μm nylon mesh) and rinsed three times with PBS, 10 μL of the collected suspension was cultured after serial dilutions on agar plates at 37 °C. After 24 h, CFU mL^{-1} of the homogenized cornea was quantified.

Histological assessment. Corneas were fixed with 4% paraformaldehyde for 24 h and embedded in paraffin to maintain the corneal structure (n = 3). Corneas were then cut into 6 μm-thick cross-sections, rehydrated, and stained with hematoxylin and eosin. Images of cross-sections of the epithelial layer around the defect were acquired with a bright-field microscope (Eclipse E800, Nikon).

Statistical analysis

All experiments were tested at least 3 times, and generated data were expressed as mean ± standard deviation. Data analysis was conducted using either T-test, one-way, or two-way ANOVA followed by Tukey's test or Bonferroni test ($^*p < 0.05$, $^{**}p < 0.01$, $^{***}p < 0.001$ and $^{****}p < 0.0001$) using GraphPad Prism 6.0.

Results and discussion

The cornea is the transparent part of the anterior eye segment. Its clarity is essential for vision and its integrity is critical for the protection of the eye against microbial pathogens. In our recent work, we developed an adhesive hydrogel, GelCORE, which can be used to properly seal and promote healing of corneal defects and ulcers from inflammation, infection, or immune disorders. We showed the efficacy and use of the engineered bioadhesive both *in vitro* and *in vivo*.[12] Incorporating a drug delivery system in this bioadhesive is critical, in particular, for infection control

and suppression of inflammation. Therefore, in the current study, we focus on the development of a drug-loaded bioadhesive which permits us to deliver CPX as a model drug into the eye. In particular, a new antimicrobial adhesive hydrogel, MC-loaded GelCORE, was designed to repair corneal wounds and prevent infection (Fig. 1). First, CPX was encapsulated in MCs to overcome its pH-dependent solubility. Secondly, GelMA, a photocrosslinkable adhesive biopolymer, was synthesized from porcine gelatin based on our previous work on the development of GelCORE.[12] MC-loaded GelCORE formulation was then formed by photocrosslinking of the prepolymer solution containing different concentrations of CPX MCs in the presence of Eosin Y (photoinitiator), TEA (co-initiator), and VC (co-monomer). The engineered MC-loaded GelCORE bioadhesives were evaluated using different chemical, mechanical, physical, antimicrobial, and cytotoxicity tests.

Characterization of CPX-loaded MCs

MCs are simple nanosystems that are usually used to improve drug solubility. The simplicity of MCs fabrication is dependent on the self-assembled structure of the used surfactant, where hydrophobic parts are oriented in the middle, forming the MCs' core and hydrophilic parts are oriented outward to the external environment as shown in Fig. 2a. In the current study, PL127 was used as a non-ionic copolymer surfactant. PL127 is a poly(ethylene oxide)–poly(propylene oxide)–poly(ethylene oxide) triblock copolymer with hydrophilic–lipophilic balance ranged from 18 to 23.[17,28] PL127 was used as a non-ionic biocompatible triblock copolymer surfactant to encapsulate CPX,

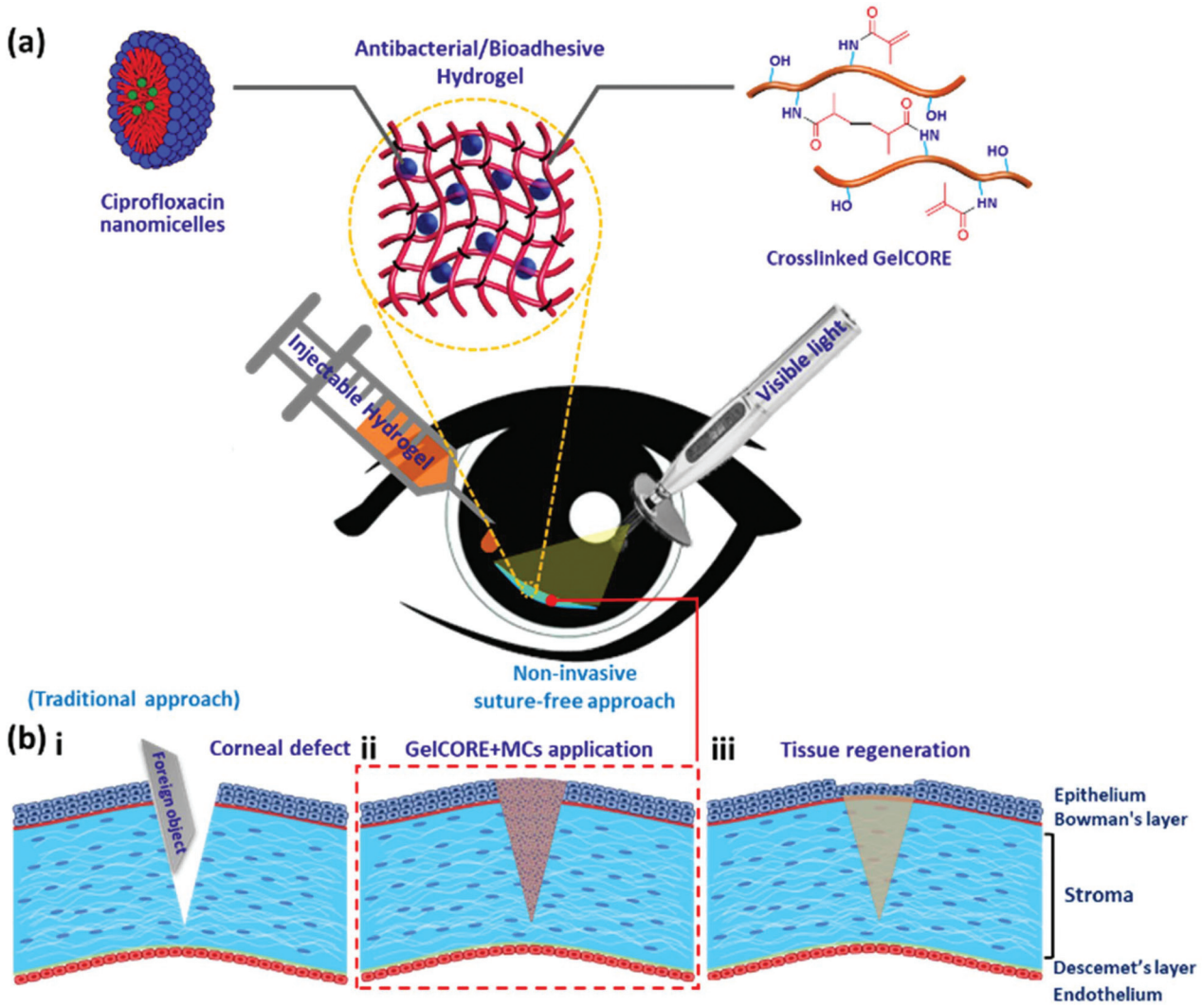

Fig. 1 Schematic of our non-invasive approach for the treatment of corneal injury with infection. (a) Schematic for the application of MC-loaded GelCORE adhesive as a suture-free approach. MC-loaded GelCORE (antibacterial bioadhesive hydrogels) was formed by photocrosslinking the prepolymer solution in the presence of Eosin Y (photoinitiator), TEA (co-initiator), and VC (co-monomer). (b) Schematic illustration of MC-loaded GelCORE application for corneal tissue regeneration after injury with a sharp object, which includes (i) the formation of a corneal laceration, (ii) application of MC-loaded GelCORE, and (iii) regeneration of the epithelial layer and stromal regeneration.

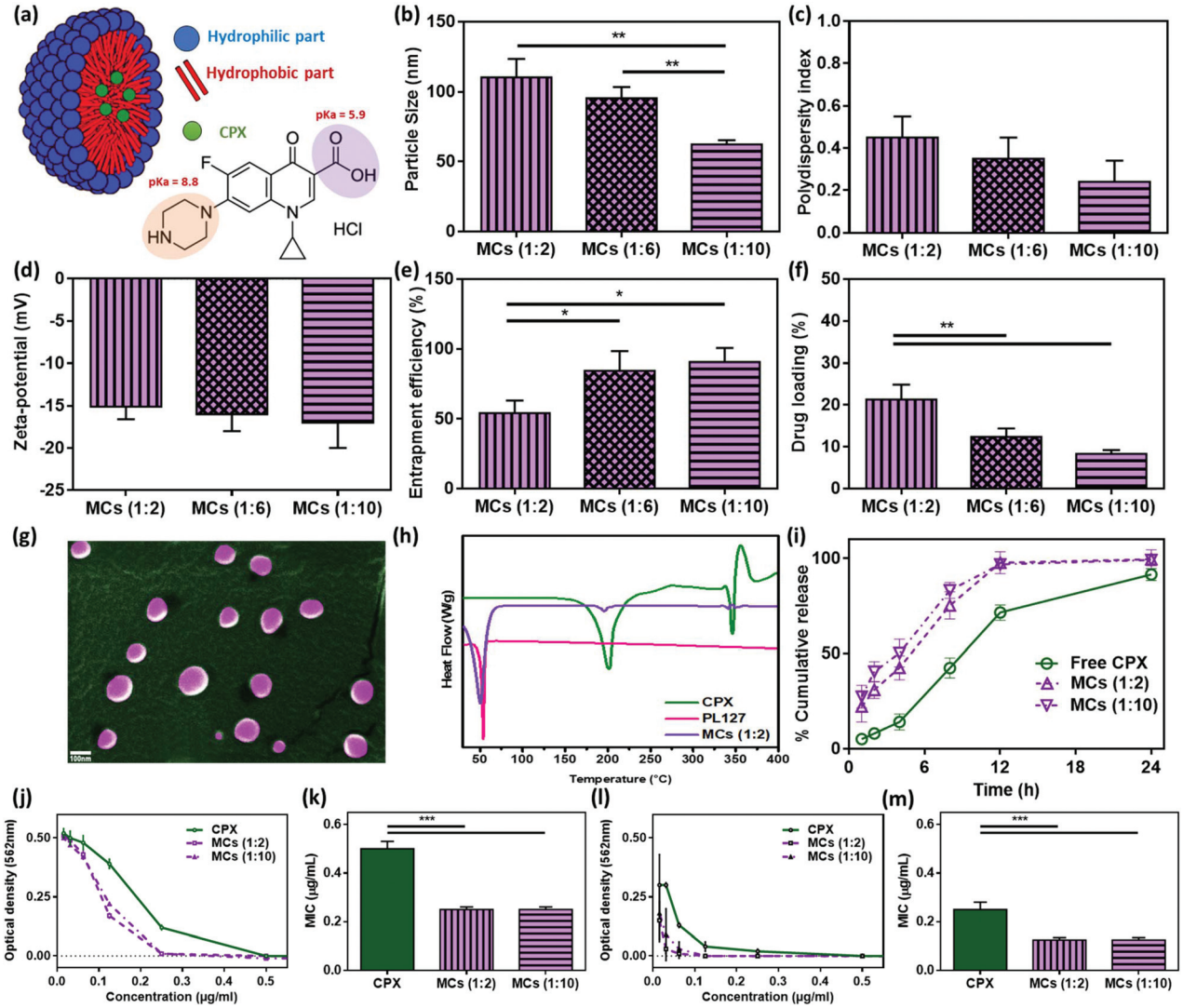

Fig. 2 Development of ciprofloxacin (CPX)-loaded micelles (MCs). (a) Graphical illustration of MCs, CPX (green) was loaded and surrounded by the hydrophobic (red) and hydrophilic (blue) elements of the MCs, the chemical structure of CPX showing the main functional groups (carboxylic and piperazine ring). (b) Average particle size, (c) polydispersity index, (d) zeta potential, (e) entrapment efficiency, and (f) drug loading for different MCs formulations. (g) A representative scanning electron microscope (SEM) image of MCs (1 : 2) (scale bar = 100 nm). (h) Differential scanning calorimetry thermograms, indicating the successful loading of ciprofloxacin inside MCs where the intensity of ciprofloxacin peaks decreased. (i) Effect of encapsulation of CPX inside the MCs on *in vitro* release profile in DPBS (pH 7.4) and 0.05% Tween 20. (j–m) Effect of MC formulation on *in vitro* antibacterial activity on *Staphylococcus aureus*: (j) optical density at a different concentration as dose–response (inhibition) curve, and (k) comparison between free drug and loaded *via* minimum inhibitory concentration curve, and on *Pseudomonas aeruginosa*: (l) optical density at a different concentration as dose–response (inhibition) curve, and (m) comparison between free drug and loaded *via* minimum inhibitory concentration curve. Data are represented as mean ± SD (*$p < 0.05$, **$p < 0.01$, ****$p < 0.0001$ and $n = 3$).

forming CPX-loaded MCs (Fig. 2a). Different CPX : PL127 ratios (1 : 2, 1 : 6 and 1 : 10) were tested. Increasing PL127 concentration significantly decreased the size of MCs from 110.34 ± 13 nm (for 1 : 2 ratio) to 62.36 ± 3 nm (for 1 : 10 ratio) (Fig. 2b). Increasing PL127 concentration also decreased the PDI from 0.45 (for 1 : 2 ratio) to 0.24 (for 1 : 10 ratio) (Fig. 2c), suggesting a better homogeneity of the colloidal system. As expected, the zeta potential of MCs showed no significant changes by varying CPX : PL127 ratio due to the non-ionic property of PL127 (Fig. 2d). Furthermore, increasing PL127 concentration significantly enhanced entrapment efficiency from 52.2 ± 9% (for 1 : 2 ratio) to 90.66 ± 10% (for 1 : 10 ratio) (Fig. 2e). This is mainly due to an increase in the amount of surfactant, that was used to encapsulate CPX, inside the system. This data is in agreement with a previous report by Abdelbary *et al.*, where Olanzapine, a hydrophobic antipsychotic drug, was encapsulated in Pluronic-based MCs.[29] In this study, the entrapment efficacy improved from 10.28 ± 2.67% to 72.92 ± 2.36% by increasing the Pluronic ratio from 1 : 20 to 1 : 40, receptively. It was also found that increasing PL127 concentration significantly decreased the drug loading percentage per micelle (Fig. 2f).

The spherical shape of the developed CPX-loaded MCs was successfully confirmed by SEM (Fig. 2g). This morphology is in agreement with a previous report by Shokry *et al*. 2019, where phenytoin, a hydrophobic anti-epileptic drug, was encapsulated in MCs.[30] Furthermore, thermal studies were conducted to confirm the encapsulation of CPX into MCs by studying the effect of heat flow as a function of temperature (Fig. 2h). CPX showed two main endothermic peaks at 205.1 °C and 345.3 °C and an exothermic peak at 354.3 °C.[31] Moreover, PL127 exhibited an endothermic peak of 60.6 °C.[30] CPX-loaded MCs (1 : 2) did not show any CPX characteristic peaks, which confirmed the successful loading of CPX in the PL127 matrix.[22]

An *in vitro* release study was conducted to investigate the rate of CPX release in a sink condition environment where drug solubility is not a rate-limiting step. The release profiles of free CPX and CPX-loaded MCs (1 : 2 and 1 : 10) were measured (Fig. 2i). Free CPX was completely solubilized within 24 h, but at a slower rate. On the other hand, both formulation of MCs completely released the drug within 12 h. For successful eradication of the infecting microorganism, the antimicrobial drug must be available on the infected site with a concentration higher than the MIC of the drug. Therefore, improving the CPX release rate after encapsulation in MCs can maintain CPX concentration above its MIC. This makes these formulations suitable candidates for engineering antimicrobial hydrogels with a fast drug release profile. Generally, antimicrobial drugs can either kill microorganisms or prevent them from thriving. This mainly depends on the dosage and frequency of drug administration. For the treatment of corneal ulcers, CPX eye drops should be applied day and night, where the frequency should be every 15 min the first day and every 4 h after day three. This course usually continues for 21 days. On the other hand, the course of treatment reduces to two days in cases of trauma, only to prevent microorganisms from spreading. CPX release profiles (Fig. 2i) were examined against different kinetic models, such as zero order, first order, Higuchi, Korsmeyer–Peppas, Hixson-Crowell, and Hopfenberg. It was found that the CPX release profile fit (r^2 0.97) to the Hixson-Crowell model ($F = 100 \times [1 - (1 - k_{HC} \times t)^3]$) where k_{HC} was 0.05 for both MCs ratios.[32]

The dose–response (inhibition) curve was plotted for *Staphylococcus aureus* (Gram-positive bacteria) in Fig. 2j to determine the MIC using a microdilution test. It was found that CPX-loaded MCs were more effective than free CPX since even lower concentrations of CPX-loaded MCs showed better inhibition as compared to free CPX. CPX MIC was determined as 0.5 μg mL^{-1} (Fig. 2k), which is in agreement with Maleki Dizaj *et al.*[33] Encapsulation of CPX in MCs significantly decreased ($p < 0.001$) MIC to 0.25 μg mL^{-1}. This could be attributed to two suggested mechanisms: (i) PL127 could alter lipid bilayer membrane structures resulted in changes to micro-viscosity; or (ii) PL127 inhibited the drug efflux transporter, leading to drug accumulation in the bacteria cells.[34] To the same extent, the dose–response (inhibition) curve was plotted for *Pseudomonas aeruginosa* (Gram-negative bacteria) as shown in Fig. 2l, showing MIC of CPX to be around 0.25 μg mL^{-1}.[35] The encapsulation of CPX significantly decreased ($p < 0.001$) the MIC value to 0.125 μg mL^{-1}. There are several reports supporting decreases in MIC when antibiotics were conjugated with polymers,[36] or encapsulation in nanosystems[37,38] to improve antimicrobial activity. The MCs prepared with 1 : 10 CPX : PL127 ratio showed the smallest particle size, the best homogeneity, and the highest entrapment efficiency. Therefore, MCs 1 : 10 was selected to be loaded into GelCORE hydrogels.

Characterization of MCs-loaded GelCORE hydrogels

GelCORE hydrogels were prepared as described previously (ESI Fig. 1a†).[12,39] ^{1}H-NMR (500 MHz; D_2O) analysis was used to confirm the methacrylation of GelMA (ESI Fig. 1b†). The appearance of peaks at δ = 5.3 ppm, 5.7 ppm, and 5.9 ppm corresponding to C=C in the structure of methacrylate and methacrylamide groups confirmed conversion of gelatin to GelMA. Furthermore, corresponding peaks of methylene lysine protons (2H) around δ = 2.8 ppm disappeared during the conversion of gelatin to GelMA supported the consumption of lysine in reaction with methacrylic anhydride. These findings are in agreement with previous reports.[6,18,33,34] After GelMA synthesis, a hydrogel was formed by mixing GelMA with TEA and VC, and Eosin Y.[40]

To prepare MC-loaded GelCORE bioadhesives, MCs and GelMA were mixed simultaneously with TEA and VC before photocrosslinking. SEM imaging was conducted to qualitatively assess the morphology of hydrogel. Incorporation of MCs (1 : 2) nano-sized delivery system did not alter the microstructure of the hydrogel networks (ESI Fig. 1c and d†), which is in agreement with Saleh *et al*. 2019.[24]

The effect of loading MCs in GelCORE hydrogels was assessed by comparing the physical characterization of GelCORE hydrogels and MC-loaded GelCORE hydrogels (GelCORE + MCs). The mechanical properties were compared through tensile and compression tests (Fig. 3a–c, ESI Fig. S2†). No significant difference was found in terms of extensibility and compressive modulus between GelCORE and GelCORE + MCs (Fig. 3b and ESI Fig. S2†). However, the loading of MCs significantly decreased the elastic modulus from 71 ± 5.9 kPa to 28.37 ± 12.1 kPa ($p < 0.001$) (Fig. 3a). Similarly, the ultimate stress of GelCORE hydrogels decreased from 70.33 ± 7.23 kPa to 36.4 ± 3.38 kPa after the addition of MCs (Fig. 3c). These results showed the loading of MCs decreased the resistance to the deformation of GelCORE hydrogels.

In addition to mechanical characterization, the swelling ratio and degradation rate were also evaluated. The addition of MCs significantly decreased ($p < 0.05$) the swelling of GelCORE hydrogels in DPBS after 24 h (Fig. 3d). For degradation tests, results showed a significant increase ($p < 0.001$) in the degradation of GelCORE + MCs over 7 days as compared with GelCORE hydrogels (Fig. 3e). These results showed that the loading of MCs changed the physical properties of GelCORE hydrogels in terms of resistance to deformation, swellability, and resistance to biodegradation, which can be

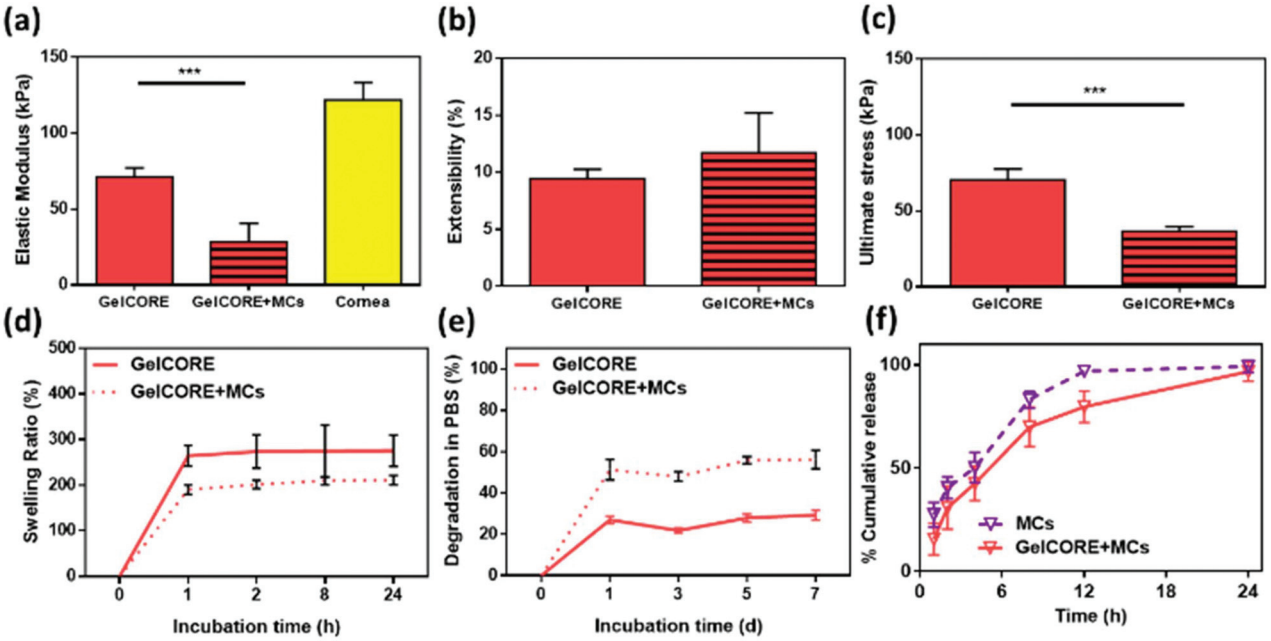

Fig. 3 *In vitro* characterization of MC-loaded GelCORE hydrogels. Mechanical characterization of GelCORE and GelCORE + MCs: (a) elastic modulus, (b) extensibility, (c) ultimate tensile strength, and (d) *In vitro* swelling ratio in DPBS for GelCORE and GelCORE + MCs. (e) *In vitro* degradation in DPBS of GelCORE and GelCORE + MCs. (f) *In vitro* release study in DPBS for CPX loaded in MCs (1 : 10) and GelCORE + MCs (1 : 10). Data are represented as means ± SD (***$p < 0.001$; $n = 3$).

explained by a lower concentration of GelMA in the GelCORE hydrogels due to the presence of MCs.

In vitro release profile was obtained in DPBS containing 0.05% Tween 20 using a dialysis membrane technique at 277 nm. Hydrogels containing CPX-loaded MCs showed similar profile to MCs (Fig. 3f). Almost ~80% of CPX was released within 12 h and ~100% within 24 h. In addtion, the CPX release profile from MCs incorporated in GelMA hydrogel was similar to the CPX release profile from CPX-loaded MCs. The kinetics of the release was examined against different models. It was found that the CPX release profile fit (r^2 0.98) to the Hixson-Crowell model ($F = 100 \times [1 - (1 - k_{HC} \times t)^3]$), where k_{HC} was 0.037 for both hydrogels.[32] This could be correlated to the degradation data, where GelMA with MCs revealed ~50% weight loss due to the diffusion of MCs from the hydrogel matrix. Therefore, the MCs could control the release of CPX from the matrix. This pattern is in agreement with a previous report by Shokry *et al.* 2019, where phenytoin MCs were incorporated in the crosslinked chitosan matrix without significant changes in the release profile.[41]

Adhesive properties of MC-loaded GelCORE hydrogels

Adhesion is another important property of the bioadhesive materials. During the wound healing process, the adhesion of the hydrogel matrix to defected tissue is vital, where most hydrogels act as a scaffold for supporting cell migration, attachment, and eventually potential biointegration.[42] Also, the bioadhesive hydrogel can be used as a matrix for CPX delivery directly to the site of infection. This cannot be achieved by currently available CPX eye ointments, where the ointment is washed out in a short amount of time after application. Herein, different adhesion tests were examined, including *in vitro* burst pressure, wound closure, and *ex vivo* tests according to ASTM standards (Fig. 4). In all experiments, the prepolymer solution of MC loaded/unloaded GelCORE was applied followed by visible light photocrosslinking. As shown in a previous study, GelCORE hydrogels exhibited high adhesive properties to the corneal tissue, making them suitable for the closure of eye injuries.[12] We assessed the effect of MCs loading on the adhesive properties of GelCORE hydrogels. For this assessment, different biological substrates (collagen sheet, rabbit corneal tissue, and whole eyeball) was used (Fig. 4).

Burst pressure tests were used to measure the ability of the adhesive hydrogel to seal a standardized defect, while airflow was applied as demonstrated in Fig. 4a and c, according to the modified ASTM standard test (F2392-04). Different substrates were used as biological tissues for burst pressure tests including collagen sheets (Fig. 4a) and rabbit corneal tissue (Fig. 4c). The burst pressures of GelMA with/without CPX-loaded MCs showed no significant changes with values around ~35 kPa in which collagen sheets were used as substrate (Fig. 4b). On the other hand, rabbit corneal tissue showed a similar pattern for GelCORE and GelCORE + MCs (around 60 kPa and 40 kPa) for 2 and 4 mm incisions, respectively (Fig. 4d). Generally, increasing incision size directly decreased burst pressure, where the average values were 56 ± 7.5 kPa for 2 mm, 32 ± 9.2 kPa for 4 mm, 14.8 ± 3.6 kPa for 6 mm, and 4.8 ± 1.2 kPa for 8 mm.

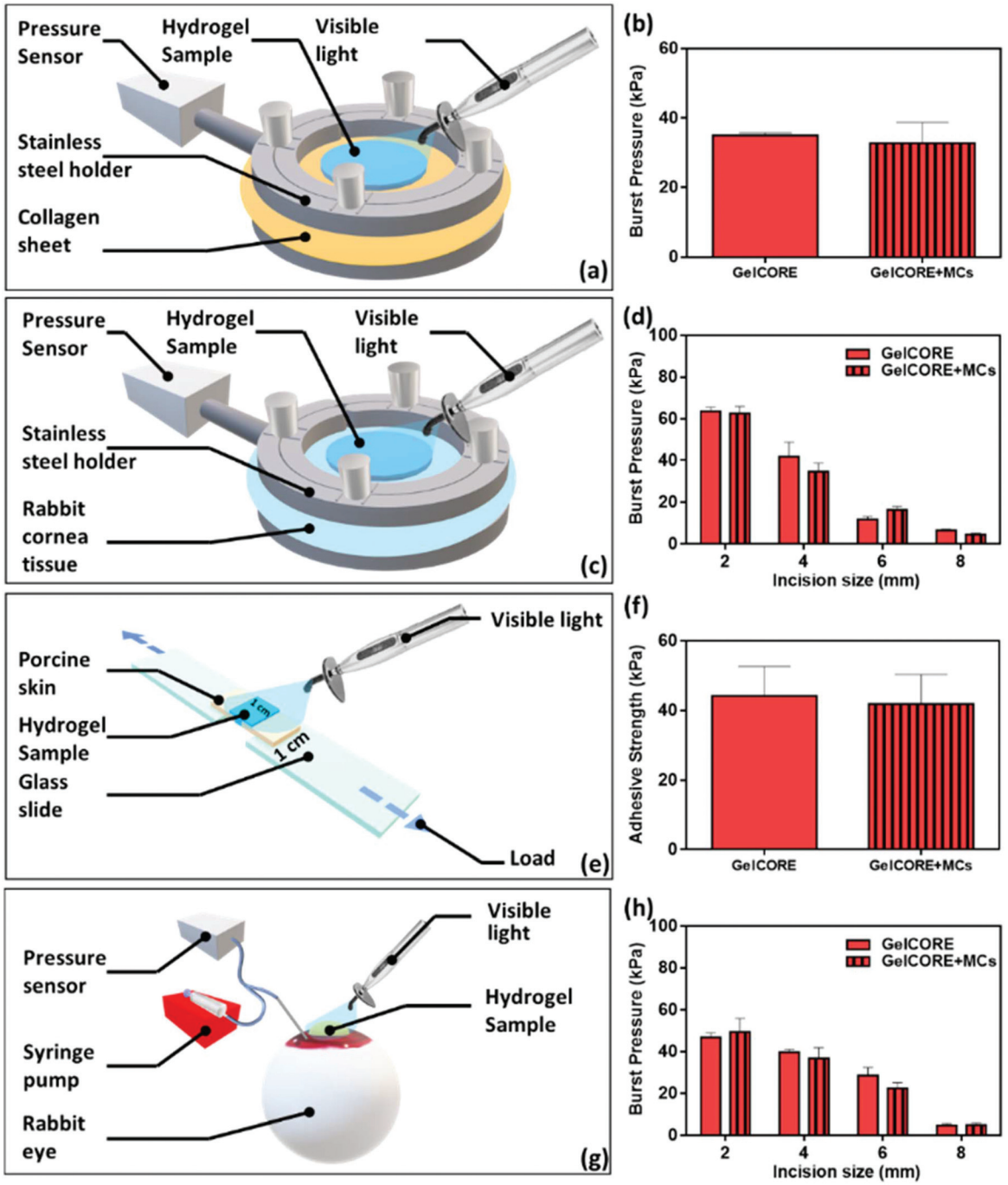

Fig. 4 Adhesive properties of GelCORE + MCs bioadhesives. (a) Schematic of a modified burst pressure test using collage sheet, and (b) average burst pressure of GelCORE and GelCORE + MCs. (c) Schematic of modified burst pressure test using corneal tissue as a biological substrate, and (d) average burst pressure. (e) Schematic of modified wound closure test using porcine skin, and (f) average adhesive strengths. (g) Schematic of *ex vivo* burst pressure test using rabbit eye ball, and (h) average burst pressure. Data are represented as means ± SD (n = 3).

Cyanoacrylate glue is usually used in corneal incision repair, which has burst pressures around 68 kPa as reported by Lauto *et al.* 2008.[43] Although cyanoacrylate glue has comparable data, it mainly works on dry surfaces and shows cytotoxicity to mammalian cells.[44]

Wound closure tests were used to measure the adhesion strength according to the modified ASTM standard (F2458-05) as shown in Fig. 4e. This test shows the ability of the hydrogel to connect the wound edges upon applying tensile stress. The incorporation of MCs inside GelCORE did not alter the adhesive strength of the hydrogels (Fig. 4f). GelCORE bioadhesives exhibited a high adhesion to different types of substrates (collagen sheet, rabbit cornea, and porcine skin) due to mechanical interlocking and covalent bonding between GelMA

and the substrate surface.[45] As shown in Fig. 4f, the adhesion strength for both GelCORE and GelCORE + MCs was around 40 kPa.

An *ex vivo* test was performed by using the whole rabbit eye with laceration with different incision sizes (Fig. 4g). A similar pattern was observed for GelMA bioadhesives with and without MCs (Fig. 4h). Generally, increasing incision size directly decreased the burst pressure, where the average burst pressures were 47.2 ± 4.9 kPa for 2 mm, 38.3 ± 3.3 kPa for 4 mm, 24 ± 3.5 kPa for 6 mm, and 3.7 ± 1.4 kPa for 8 mm. Therefore, all adhesion tests demonstrated that both GelCORE and GelCORE + MCs formulations had similar adhesion characteristics. Results demonstrated no significant difference in burst pressures between GelCORE and GelCORE + MCs regardless of the substrate used or the injury size. This suggests that loading of MCs maintained the adhesive properties of GelCORE hydrogels.

In vitro antimicrobial study on MCs-loaded GelCORE hydrogels

Staphylococcus aureus and *Pseudomonas aeruginosa* are common causes of eye infections. Therefore, these two bacterial strains were used to test the antibacterial activity of the hydrogels. Agar diffusion tests were performed to compare the antibacterial properties GelCORE and GelCORE + MCs hydrogels (Fig. 5).

First, the zone of inhibition studies was used to compare the effect of free CPX, CPX-loaded MCs, GelCORE, and GelCORE + MCs after 24 h (Fig. 5a–d). According to the dose–response curve, the MIC of CPX was 0.5 μg mL^{-1} and 0.25 μg mL^{-1} for *Staphylococcus aureus* and *Pseudomonas aeruginosa*, respectively. While, MIC of CPX loaded MCs (1 : 10) was 0.25 μg mL^{-1} and 0.125 μg mL^{-1} for *Staphylococcus aureus* and *Pseudomonas aeruginosa*, respectively (Fig. 1j–m). The zone of inhibition test was conducted using the MIC of CPX and MCs (1 : 10). For *Staphylococcus aureus*, data showed no significant difference between CPX (44.6 mm) and loaded MCs (46.1 mm) as both tests were conducted at their MIC concentrations, as shown in Fig. 5e. Moreover, a significant increase in inhibition zone was observed in GelCORE + MCs. The values were 21.9 mm and 35.5 mm for GelCORE and GelCORE + MCs, respectively. It worth mentioning that the inhibition zone of GelCORE + MCs was ~20% less than CPX-loaded MCs. This could be correlated to the nature of the inhibition zone test, where solid agar is used, and MCs required enough liquid media to migrate from the hydrogel to reach the agar. This is in agreement with Alvarez *et al.* 2014 study,[46] where rifamycin loaded silica-collagen nanocomposite hydrogels showed unmatched antibacterial activity. Rifamycin was strongly adsorbed into nanocomposite hydrogels without inhibition of *Staphylococcus aureus* and *Pseudomonas aeruginosa.* The bacterial viability assay was also used to visually confirm bacterial inhibition using the LIVE/DEAD® BacLight™ kit (Fig. 5f and g). It is clear from the images that GelCORE kept bacteria alive (green stain) as shown in Fig. 5f, while GelCORE + MCs almost eradicated (red stain) all *Staphylococcus aureus* cells (Fig. 5g).

To the same extent, inhibition zone tests against *Pseudomonas aeruginosa* was conducted with previously men-

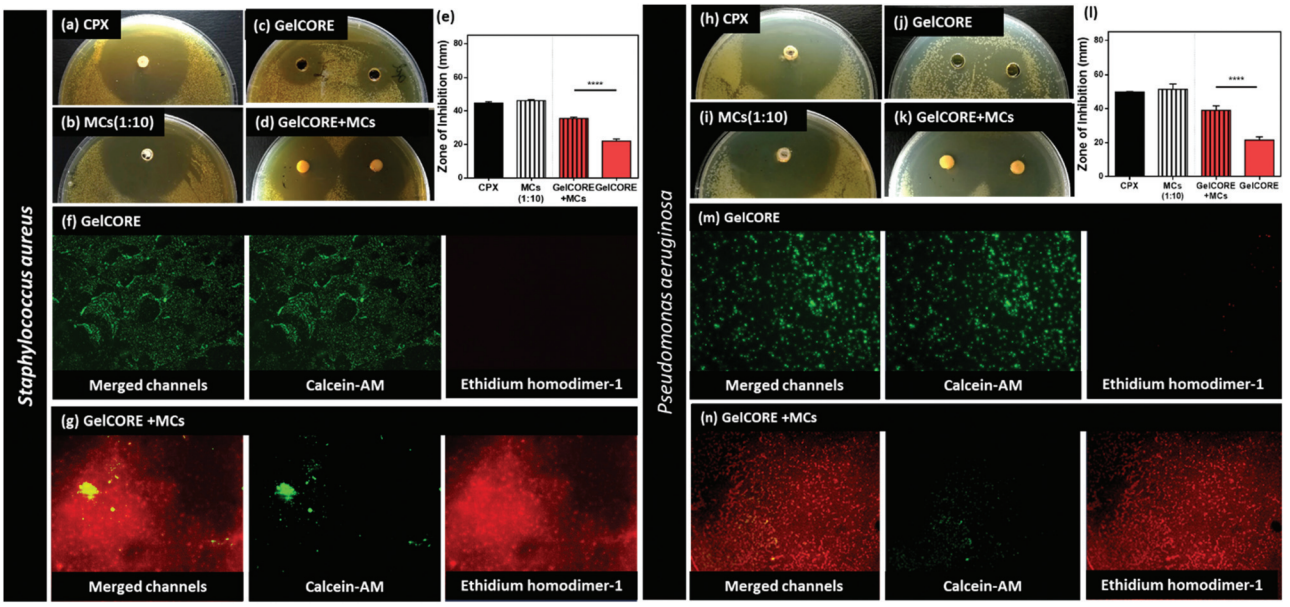

Fig. 5 *In vitro* microbiological properties of MC-loaded GelCORE hydrogels. Zone of inhibition study on *Staphylococcus aureus* for (a) ciprofloxacin (CPX), (b) ciprofloxacin micelles (MCs), (c) GelCORE, and (d) GelCORE + MCs. (e) Average zone of inhibition of different samples. Bacterial viability assays using LIVE/DEAD® BacLight™ kit on *Staphylococcus aureus* for (f) GelCORE, and (g) GelCORE + MCs. Zone of inhibition study on *Pseudomonas aeruginosa* for (h) CPX, (i) CPX MCs, (j) GelCORE, (k) GelCORE + MCs. (l) Average zone of inhibition of different samples. Bacterial viability assays using LIVE/DEAD® BacLight™ kit on *Pseudomonas aeruginosa* for (m) GelCORE, and (n) GelCORE + MCs. Data are represented as means ± SD (****$P < 0.0001$; $n = 3$).

tioned MICs (Fig. 5h–k). No significant difference between CPX (49.7 mm) and loaded MCs (51.4 mm) was observed as both tests were conducted at its MIC concentration as shown in Fig. 5l. Moreover, a significant increase in inhibition zone was observed for GelCORE + MCs. The values were 21.5 mm and 39 mm for GelCORE and GelCORE + MCs, respectively. Also, the bacterial viability assay was conducted (Fig. 5m and n). GelCORE bioadhesive kept bacteria alive (green stain) as shown in Fig. 5m, while GelCORE + MCs eradicated (red stain) almost all *Pseudomonas aeruginosa* cells (Fig. 5n).

Our study aimed to prevent infection through improving the delivery of CPX to an infected corneal wound. Several attempts have used nanocomposite hydrogels to treat different types of infected wounds. For example, CPX and silver nanoparticles were stabilized in guar gum alkyl amine to obtain a nanocomposite as a dual-component drug delivery system. The developed nanocomposite demonstrated supportive effects against *Pseudomonas aeruginosa*, *Escherichia coli*, *Bacillus cereus*, and *Staphylococcus aureus*.[47] Another study developed CPX and tripeptide dual loaded hydrogel activity against *Staphylococcus aureus*, *Escherichia coli*, and *Klebsiella pneumonia*.[48] So, many previous reports supported current study findings, where MC-loaded GelMA as a nanocomposite hydrogel has a suitable antibacterial activity against both grams positive and Gram-negative bacteria. These results suggest that MC-loaded GelCORE hydrogels represent a suitable delivery system for CPX and can provide antibacterial activity against Gram-positive and Gram-negative bacterial strains.

In vitro cytocompatibility of GelCORE + MCs hydrogels

In vitro cytocompatibility of GelCORE and GelCORE + MCs bioadhesive was compared by cell viability, adhesion/spreading, and proliferation tests using corneal fibroblast cells (Fig. 6). Cell viability was determined using a live/dead assay at different post-seeding time points (days 1, 4, and 7) as shown in Fig. 6a–f. No significant difference in cell viability was observed between GelCORE and GelCORE + MCs hydrogels (Fig. 6m). Actin/DAPI staining also showed no significant differences in the adhesion and spreading of the cells cultured on GelCORE and GelCORE + MCs hydrogels (Fig. 6g–l). Finally, no difference in terms of proliferation was observed between GelCORE and GelCORE + MCs hydrogels (Fig. 6n). These results suggest that the loading of MCs did not affect the cytocompatibility of GelCORE hydrogels.

Ex vivo efficiency of GelCORE + MCs hydrogels

An *ex vivo* infectious pig corneal defect model was used to assess the efficacy of GelCORE + MCs as compared with GelCORE. A 6 mm stromal defect was created on pig eyeballs and filled with 20 μL of bioadhesive. OCT imaging confirmed that GelCORE + MCs bioadhesive was able to fill the defect and adhere to the stromal bed (Fig. 7a and b). After bacterial infection and bioadhesive application, Petri dishes containing the corneas and their surrounding media showed high turbidity for corneas not treated and corneas treated with GelCORE. However, for corneas treated with GelCORE + MCs, the surrounding medium appeared clear and comparable to the

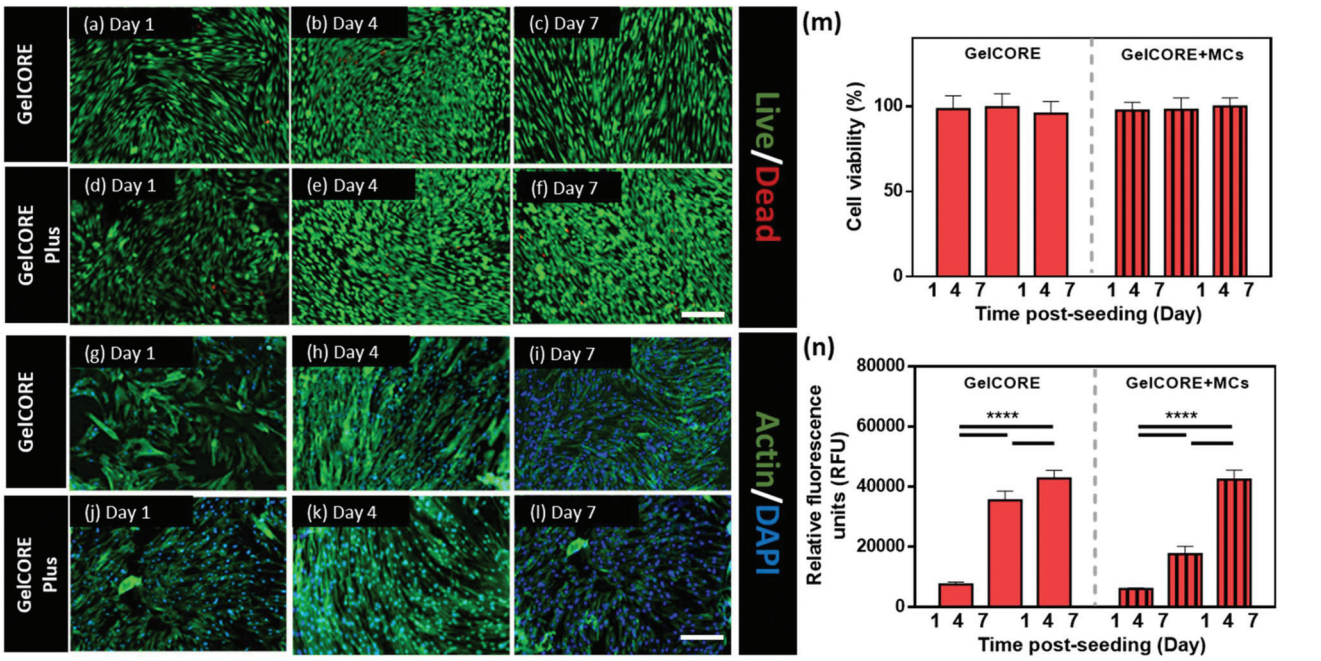

Fig. 6 *In vitro* cytocompatibility of GelCORE + MCs bioadhesive. Representative LIVE/DEAD images from corneal fibroblast cells on days 1, 4, and 7 after seeding (scale bar = 100 mm) on (a–c) GelCORE, and (d–f) GelCORE + MCs. Representative Actin/DAPI images from corneal fibroblast cells on days 1, 4, and 7 after seeding (scale bar, 100 mm) on (g–i) GelCORE, and (j–l) GelCORE + MCs. (m) Quantification of cell viability on GelCORE and GelCORE + MCs after 1, 4, and 7 days of culture. (n) Quantification of metabolic activity of corneal fibroblast cells seeded on GelCORE and GelCORE + MCs after 1, 4, and 7 days. Data are represented as means ± SD (****$P < 0.0001$; $n = 3$).

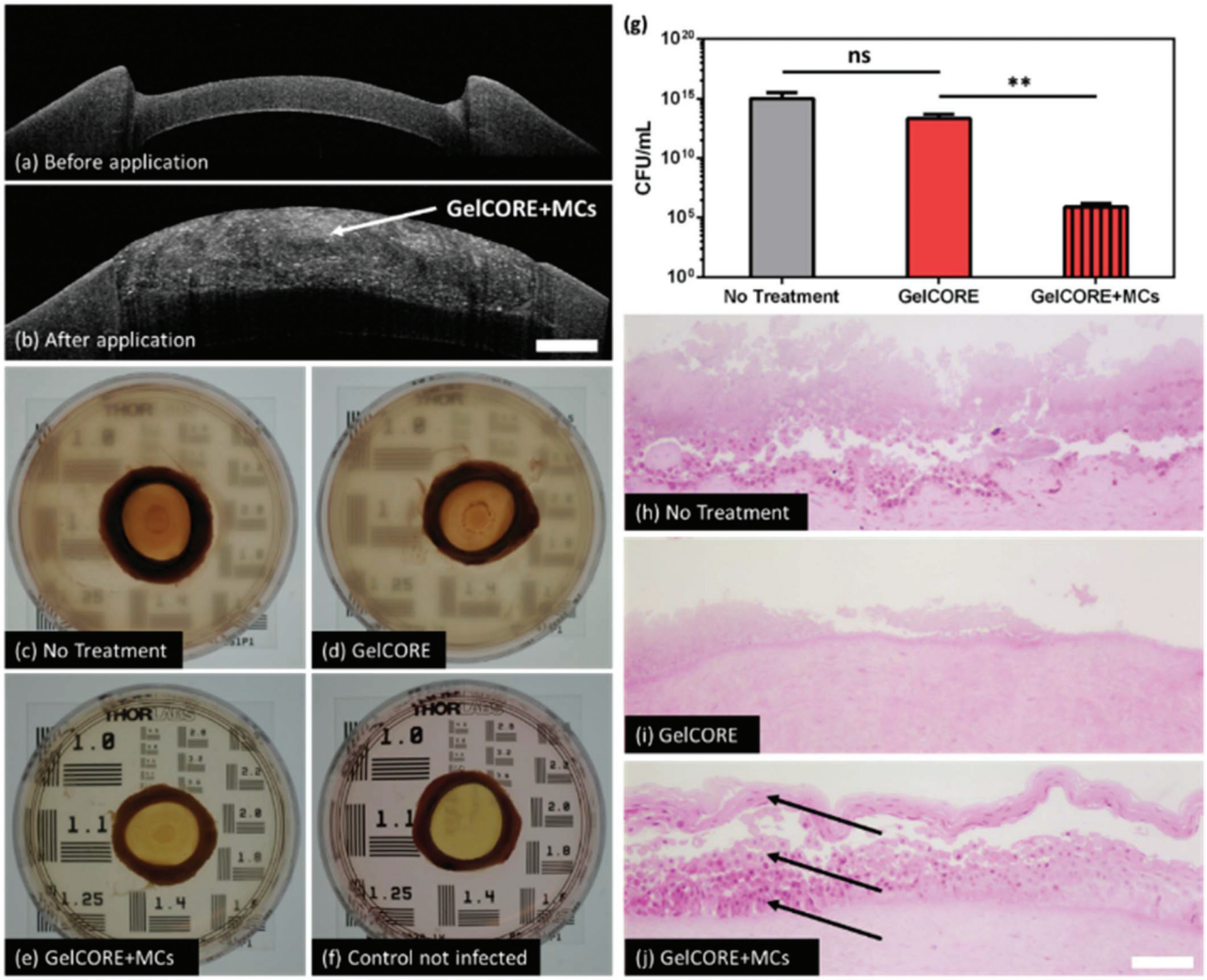

Fig. 7 *Ex vivo* studies on GelCORE + MCs bioadhesive. Representative OCT images of corneas (a) before and (b) after GelCORE + MCs application (scale bar = 1 mm). Representative top-view images of corneas infected with *Pseudomonas aeruginosa* and (c) not treated, (d) treated with GelCORE, (e) treated with GelCORE + MCs, and (f) not-infected cornea. (g) Results of CFU of the homogenized cornea of each group. Data are represented as means ± SD (**$P < 0.01$, $n = 5$). (h–j) Histological cross-sections of corneal epithelium around the defect at ×20 magnification. Arrows show the three different layers (basal, wing, and squamous cells) constituting healthy corneal epithelium (scale bar = 50 μm).

control corneas that were infected (Fig. 7c–f). Results of bacterial culture after corneal homogenization and filtration showed a significantly lower CFU count for the GelCORE + MCs group as compared with the GelCORE group and no treatment group (Fig. 7g). Finally, H&E staining showed that the corneal epithelium was found damaged for corneas treated with GelCORE and corneas not treated. For corneas treated with GelCORE + MCs, all three layers of epithelium were present, suggesting higher viability due to a lower bacterial presence (Fig. 7h–j).

The ideal biomaterial for the uses we have envisaged and discussed in this study should be biocompatible, highly adhesive, able to elute antibiotics with a predictable kinetics, and possess biomechanical properties that mimic those of the native cornea. Work in the past two decades in biomaterial applications to the eye has focused largely on unwanted wound healing responses such as the immunoinflammatory responses and angiogenesis, but very little data are available for longer term retention and performance of biomaterials. Commercialized products such as ReSure (Ocular Therapeutix Inc., MA, USA), which is a PEG-based adhesive and ocular sealant, is unable to fill stromal defects due to rapid polymerization that limits the time for material application in the defect.[12] Other research groups have focused on developing new biomaterials such as acrylate gelatin-based hydrogel,[49] collagen vitrigel,[50] fibrin,[51] gelatin,[52] alginate,[53] and chitosan[54] for eye tissue regeneration. However, there has been a lack of systematic clinical evaluation of these products, making it difficult to directly compare their performance, safety, and efficacy. Additionally, introduction of new biomaterial 'devices' into the clinical realm faces complex regulatory barriers that need to be surmounted.

Conclusions

Drug-eluting biomaterials can provide several unique advantages over conventional drug delivery systems such as site-targeted delivery, lower dosage requirements, and improved patient compliance. In this study, we developed and tested a CPX-loaded gelatin-based adhesive hydrogel for the management of corneal injuries associated with infection or risk of infection. To incorporate CPX into GelCORE hydrogels, PL127 was used as a micellar system. *In vitro* release studies demonstrated a release of CPX over 24 h with 80% of the drug release in the first 12 h. Results also showed that although the addition of MCs altered some physical properties of the GelCORE hydrogels, the adhesive properties and cytocompatibility of the MC-loaded hydrogels were well maintained. *Ex vivo* studies showed that the addition of CPX-loaded MCs in GelCORE hydrogels provided excellent antimicrobial properties by significantly decreasing bacterial levels in the corneal tissue. More interestingly, a higher corneal epithelial viability was observed for corneas treated with MC-loaded GelCORE hydrogels, confirming the hydrogel's biocompatibility and its cytoprotection of corneal cells against infection. Despite the need for *in vivo* proof-of-concept studies, this study suggests that CPX-loaded GelCORE hydrogels could represent a promising solution for the treatment of corneal injuries and preventing ocular infection. The chemistry of GelCORE hydrogels would permit the incorporation of a wide array of therapeutics. As such, the GelCORE hydrogel system could represent a promising drug eluting platform for treatment of differecnt ocular diseases.

Conflicts of interest

There are no conflicts to declare.

Acknowledgements

This work is supported by the National Institutes of Health (NIH) (R01EB023052 and R01HL140618), Department of Defense Vision Research Program Technology/Therapeutic Development Award (W81XWH-18-1-0654). We thank Dr Paulo Bispo and Maggie Lau for their help with bacterial culture and counting.

References

1 J. P. Whitcher, M. Srinivasan and M. P. Upadhyay, *Bull. W. H. O.*, 2001, **79**, 214–221.
2 M. L. Durand, *Clin. Microbiol. Rev.*, 2017, **30**, 597–613.
3 C. Jumelle, S. Gholizadeh, N. Annabi and R. Dana, *J. Controlled Release*, 2020, **321**, 1–22.
4 R. Gupta, B. Patil, B. M. Shah, S. J. Bali, S. K. Mishra and T. Dada, *J. Glaucoma*, 2012, **21**, 189–192.
5 F. Kashiwabuchi, K. S. Parikh, R. Omiadze, S. Zhang, L. Luo, H. V. Patel, Q. Xu, L. M. Ensign, H. Q. Mao, J. Hanes and P. J. McDonnell, *Transl. Vision Sci. Technol.*, 2017, **6**, 1–8.
6 M. Champeau, J.-M. Thomassin, T. Tassaing and C. Jérôme, *Expert Opin. Drug Delivery*, 2017, **14**, 1293–1303.
7 G. van Rij and G. O. W. III, *Am. J. Ophthalmol.*, 1984, **98**, 773–783.
8 P. Marone, V. Monzillo, Ç. Segù and E. Antoniazzi, *Ophthalmologica*, 1999, **213**, 12–15.
9 L. U. Lahoda, S. C. Wang and P. M. Vogt, *Chirurg*, 2006, **77**, 251–256.
10 W. Yee, G. Selvaduray and B. Hawkins, *J. Mech. Behav. Biomed. Mater.*, 2016, **55**, 67–74.
11 J. Yin, R. B. Singh, R. Al Karmi, A. Yung, M. Yu and R. Dana, *Cornea*, 2019, **38**, 668–673.
12 E. Shirzaei Sani, A. Kheirkhah, D. Rana, Z. Sun, W. Foulsham, A. Sheikhi, A. Khademhosseini, R. Dana and N. Annabi, *Sci. Adv.*, 2019, **5**, 1–14.
13 A. Smith, P. M. Pennefather, S. B. Kaye and C. A. Hart, *Drugs*, 2001, **61**, 747–761.
14 G.-F. Zhang, X. Liu, S. Zhang, B. Pan and M.-L. Liu, *Eur. J. Med. Chem.*, 2018, **146**, 599–612.
15 A. O. Surov, A. P. Voronin, K. V. Drozd, A. V. Churakov, P. Roussel and G. L. Perlovich, *CrystEngComm*, 2018, **20**, 755–767.
16 K. R. Wilhelmus and R. L. Abshire, *Am. J. Ophthalmol.*, 2003, **136**, 1032–1037.
17 E. I. Taha, M. M. Badran, M. H. El-Anazi, M. A. Bayomi and I. M. El-Bagory, *J. Mol. Liq.*, 2014, **199**, 251–256.
18 M. M. Mehanna, H. A. Elmaradny and M. W. Samaha, *Drug Dev. Ind. Pharm.*, 2009, **35**, 583–593.
19 L. Budai, M. Hajdú, M. Budai, P. Gróf, S. Béni, B. Noszál, I. Klebovich and I. Antal, *Int. J. Pharm.*, 2007, **343**, 34–40.
20 K. Dillen, W. Weyenberg, J. Vandervoort and A. Ludwig, *Eur. J. Pharm. Biopharm.*, 2004, **58**, 539–549.
21 K. P. Pagar and P. R. Vavia, *Ther. Delivery*, 2013, **4**, 553–565.
22 I. A. Khalil, I. H. Ali and I. M. El-Sherbiny, *Nanomedicine*, 2019, **14**, 33–55.
23 A. Hefnawy, I. A. Khalil and I. M. El-Sherbiny, *Nanomedicine (Lond).*, 2017, **12**(24), 2737–2761.
24 B. Saleh, H. K. Dhaliwal, R. Portillo-Lara, E. Shirzaei Sani, R. Abdi, M. M. Amiji and N. Annabi, *Small*, 2019, **15**, 1–15.
25 A. Pinnock, N. Shivshetty, S. Roy, S. Rimmer, I. Douglas, S. MacNeil and P. Garg, *Graefe's Arch. Clin. Exp. Ophthalmol.*, 2017, **255**, 333–342.
26 J. Yin and F.-S. X. Yu, *Invest. Ophthalmol. Visual Sci.*, 2010, **51**, 1891–1897.
27 D. Guindolet, E. Crouzet, Z. He, P. Herbepin, C. Jumelle, C. Perrache, J. M. Dumollard, F. Forest, M. Peoc'h, P. Gain, E. Gabison and G. Thuret, *Invest. Ophthalmol. Visual Sci.*, 2017, **58**, 5907–5917.
28 N. M. Elbaz, I. A. Khalil, A. A. Abd-Rabou and I. M. El-Sherbiny, *Int. J. Biol. Macromol.*, 2016, **92**, 254–269.
29 G. A. Abdelbary and M. I. Tadros, *Int. J. Pharm.*, 2013, **452**, 300–310.

30 M. M. Shokry, I. A. Khalil, A. El-Kasapy, A. Osman, A. Mostafa, M. Salah and I. M. El-Sherbiny, *Carbohydr. Polym.*, 2019, **223**, 1–9.
31 Z. Tan, F. Tan, L. Zhao and J. Li, *J. Cryst. Process Technol.*, 2012, **02**, 55–63.
32 P. Costa and J. M. Sousa Lobo, *Eur. J. Pharm. Sci.*, 2001, **13**, 123–133.
33 S. Maleki Dizaj, F. Lotfipour, M. Barzegar-Jalali, M.-H. Zarrintan and K. Adibkia, *Artif. Cells, Nanomed., Biotechnol.*, 2017, **45**, 535–543.
34 P. Chowdhury, P. K. B. Nagesh, S. Kumar, M. Jaggi, S. C. Chauhan and M. M. Yallapu, *Pluronic Nanotechnology for Overcoming Drug Resistance*, ed. B. Yan, H. Zhou and J. L. Gardea-Torresdey, Springer Singapore, Singapore, 2017, ch. 9, pp. 207–237.
35 R. Garhwal, S. F. Shady, E. J. Ellis, J. Y. Ellis, C. D. Leahy, S. P. McCarthy, K. S. Crawford and P. Gaines, *Invest. Ophthalmol. Visual Sci.*, 2012, **53**, 1341–1352.
36 M. Schmidt, S. Harmuth, E. R. Barth, E. Wurm, R. Fobbe, A. Sickmann, C. Krumm and J. C. Tiller, *Bioconjugate Chem.*, 2015, **26**, 1950–1962.
37 E. Turos, J.-Y. Shim, Y. Wang, K. Greenhalgh, G. S. K. Reddy, S. Dickey and D. V. Lim, *Bioorg. Med. Chem. Lett.*, 2007, **17**, 53–56.
38 N. Günday Türeli, A. Torge, J. Juntke, B. C. Schwarz, N. Schneider-Daum, A. E. Türeli, C.-M. M. Lehr and M. Schneider, *Eur. J. Pharm. Biopharm.*, 2017, **117**, 363–371.
39 M. Uehara, X. Li, A. Sheikhi, N. Zandi, B. Walker, B. Saleh, N. Banouni, L. Jiang, F. Ordikhani, L. Dai, M. Yonar, I. Vohra, V. Kasinath, D. P. Orgill, A. Khademhosseini, N. Annabi and R. Abdi, *Sci. Rep.*, 2019, **9**, 1–13.
40 H. Shirahama, B. H. Lee, L. P. Tan and N.-J. Cho, *Sci. Rep.*, 2016, **6**, 1–11.
41 M. M. Shokry, I. A. Khalil, A. El-Kasapy, A. Osman, A. Mostafa, M. Salah and I. M. El-Sherbiny, *Carbohydr. Polym.*, 2019, **223**, 1–9.
42 D.-A. Wang, S. Varghese, B. Sharma, I. Strehin, S. Fermanian, J. Gorham, D. H. Fairbrother, B. Cascio and J. H. Elisseeff, *Nat. Mater.*, 2007, **6**, 385–392.
43 A. Lauto, D. Mawad and L. J. R. Foster, *J. Chem. Technol. Biotechnol.*, 2008, **83**, 464–472.
44 G. Ciapetti, S. Stea, E. Cenni, A. Sudanese, D. Marraro, A. Toni and A. Pizzoferrato, *Biomaterials*, 1994, **15**, 63–67.
45 N. Annabi, D. Rana, E. Shirzaei Sani, R. Portillo-Lara, J. L. Gifford, M. M. Fares, S. M. Mithieux and A. S. Weiss, *Biomaterials*, 2017, **139**, 229–243.
46 G. S. Alvarez, C. Hélary, A. M. Mebert, X. Wang, T. Coradin and M. F. Desimone, *J. Mater. Chem. B*, 2014, **2**, 4660–4670.
47 G. A. Islan, A. Mukherjee and G. R. Castro, *Int. J. Biol. Macromol.*, 2015, **72**, 740–750.
48 S. Marchesan, Y. Qu, L. J. Waddington, C. D. Easton, V. Glattauer, T. J. Lithgow, K. M. McLean, J. S. Forsythe and P. G. Hartley, *Biomaterials*, 2013, **34**, 3678–3687.
49 L. Li, C. Lu, L. Wang, M. Chen, J. White, X. Hao, K. M. McLean, H. Chen and T. C. Hughes, *ACS Appl. Mater. Interfaces*, 2018, **10**, 13283–13292.
50 J. J. Chae, W. McIntosh Ambrose, F. A. Espinoza, D. G. Mulreany, S. Ng, T. Takezawa, M. M. Trexler, O. D. Schein, R. S. Chuck and J. H. Elisseeff, *Acta Ophthalmol.*, 2015, **93**, e57–e66.
51 M. Banitt, J. B. Malta, H. K. Soong, D. C. Musch and S. I. Mian, *Curr. Eye Res.*, 2009, **34**, 706–710.
52 J. Rose, S. Pacelli, A. Haj, H. Dua, A. Hopkinson, L. White and F. Rose, *Materials*, 2014, **7**, 3106–3135.
53 D. N. Mishra and R. M. Gilhotra, *Daru, J. Pharm. Sci.*, 2008, **16**, 1–8.
54 T. Gratieri, G. M. Gelfuso, E. M. Rocha, V. H. Sarmento, O. de Freitas and R. F. V. Lopez, *Eur. J. Pharm. Biopharm.*, 2010, **75**, 186–193.